

Supplementary Information

Functionalized MIL-101(Cr) Metal-Organic Framework for Enhanced Hydrogen Release from Ammonia Borane at Low Temperature

Liang Gao, Chi-Ying Vanessa Li, Hoi Yung and Kwong-Yu Chan*

Department of Chemistry, the University of Hong Kong, Pokfulam Road, Hong Kong SAR, P.R. China.

*email:hrsccky@hku.hk.

Sample preparation

All chemicals, if not mentioned specially, were ordered form Sigma Aldrich and used without further purification. MIL-101 were synthesized in accordance to previous report under hydrothermal condition at 220°C.¹ Afterwards, the as-prepared MIL-101 was purified according to the following two steps: First, the as-prepared MIL-101 was immersed in EtOH(0.1g/10mL) and was heated in an autoclave to 100°C for 20hr; then, MIL-101 was immersed in 30mM NH₄F aqua solution for 10h at 60°C at a N₂ flow. NO₂-101 was prepared according to previous report by nitrating MIL-101 with conc.HNO₃ and H₂SO₄ mixture at 0°C.² Then, NH₂-101 was prepared by reducing NO₂-101 with SnCl₂·2H₂O dissolved in absolute EtOH.² ¹H NMR spectra confirmed the successful introduction of nitro and amino groups. Both prepared samples were dried at 150 °C in air overnight. NHCOCH₃-101 was synthesized by acylating NH₂-101 with acetic anhydride. Typically, 0.03g NH₂-101 suspended in 10mL CHCl₃ was reacted with 100uL acetic anhydride at 20 °C for a period of days. Then, the prepared NHCOCH₃-101 was centrifuged out and washed a lot with CHCl₃, EtOH and acetone. The greenish powder obtained was dried at 150 °C in air overnight. AB was loaded into the porous MIL-101s by a simple impregnation method. Typically, 0.2g 1:1 wt/wt AB/MILs (MIL-101 and covalently modified MIL-101) mixtures were immersed into 100uL anhydrous THF and kept stirring for half an hour. THF was evaporated off under dynamic vacuum at 21 °C for 12hr and gravimetric method was used to confirm the total remove of THF. The obtained dry powder was sealed into vials in a dry box and placed in refrigerator for further characterization. As control experiments, AB was also physically mixed with various MIL-101s by grinding them (1:1 wt/wt) in a mortar for 10 min.

Characterization

X-ray diffraction (XRD) patterns were obtained on a Bruker Advance D8 diffractometer with a lynxeye detector at 40 kV and 40 mA with a scanning rate of 4 °/min. The Brunauer–Emmett–Teller (BET) surface areas and porosity were measured by Micromeritics ASAP 2020 analyzer at 77 K. Each time, ~0.1 g sample was evacuated in a vacuum oven at

150 °C overnight. The sample was then transferred to preweighed quartz tube and degassed at 150 °C until the system pressure < 5 µmHg. Afterwards, the tube was reweighed to obtain an accurate mass for BET surface area determination. Fourier transform infrared spectroscopy (FTIR, Shimadzu, KBr pellet) was performed at 20 °C at a 4 cm⁻¹ resolution. Nuclear magnetic resonance (NMR) spectra of various phthalic acid derivatives were recorded on a Bruker 400M equipment. Electrospray ionization mass spectrometry (ESI-MS) was conducted on a ThermoFinnigan LCQ-DECA mass spectrometer. Before NMR testing, samples were dried under a dynamic vacuum at 150 °C overnight to remove coordinated water. Then, 10 mg dried samples were digested in 500 µL 2 wt.%NaOD/D₂O with sonication to produce a clean solution where Cr(OH)₃ was quantitatively participated as the pH was adjusted to 8~10 according to the Pourbaix diagram of Cr species.³ The hydroxides were filtered off by filter paper(Advantec, 1#), the pH of residual solution was then adjusted to 1~2 by using 20 wt.% HCl and the terephthalic acid species were extracted with anhydrous diethyl ether, which was subsequently evaporated off by a Rotavapor to obtain yellowish power for further NMR and ESI-MS characterization. Thermal gravimetric analysis(TGA) was performed at a 20 mL/min N₂ flow with a heating rate of 3 °C/min. The temperature dependence and isothermal kinetics of AB-MIL-101s samples were studied by a temperature-programmed-desorption (TPD, HidenCatlab) system with an on-line mass spectrometer (QGA, Hiden) to monitor the gaseous components. For temperature dependence mode, the temperature was increased from 37 °C to 200 °C (3 °C/min). For isothermal mode, samples were quickly (20 °C/min) heated to a given temperature and then held at this temperature for 3h.

Theoretical calculation

All calculations were performed at the MP2/6-311++G(d,p) level of theory using the *Gaussian 03* package.⁴ To simply the problems and stress our foci, the ligand NH₂-H₂BDC instead of NH₂-H₂BDC-101 is adopted to interact with AB as structures are optimized.

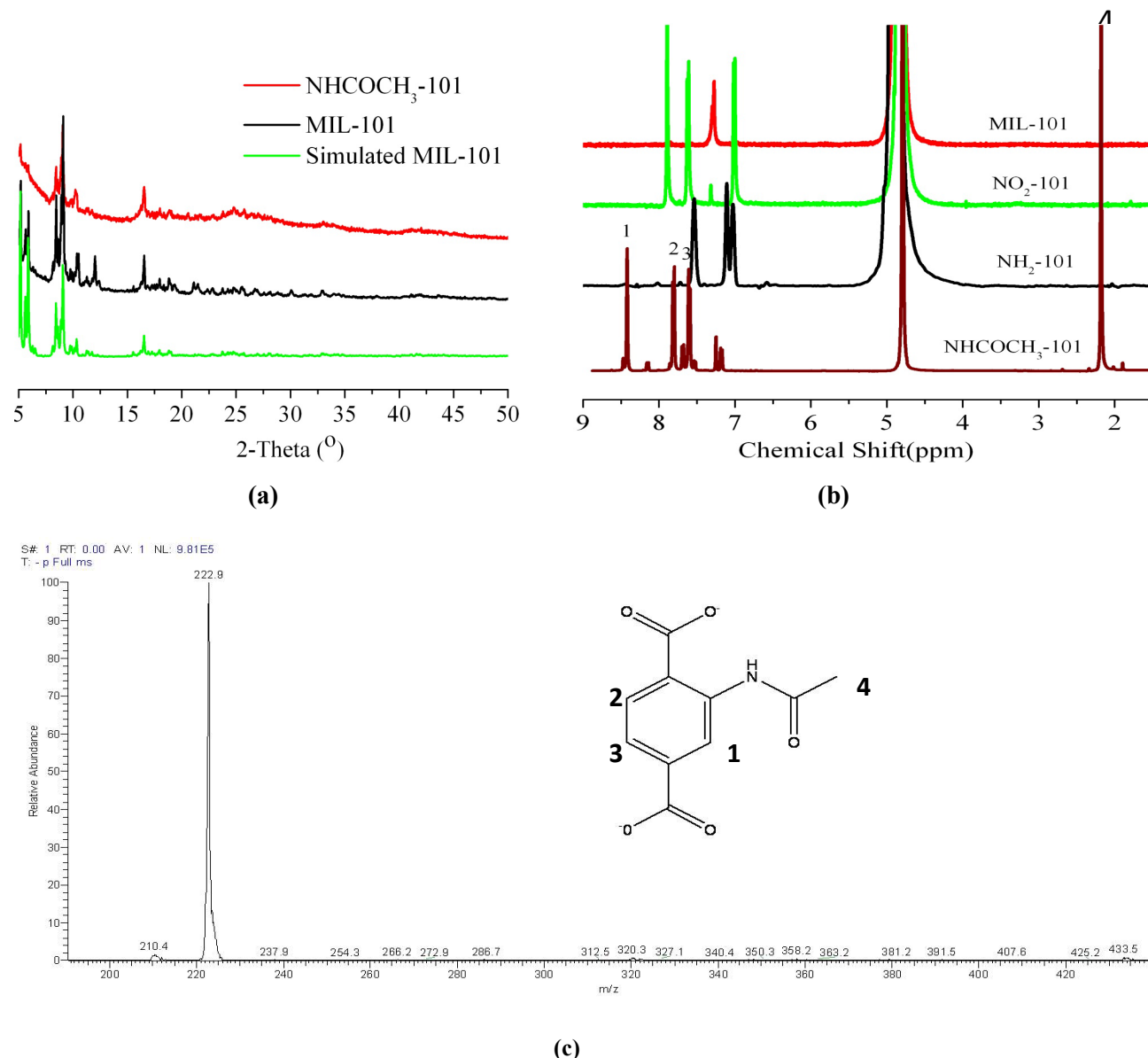


Figure S1 **a)** XRD patterns of NHCOCH₃-101, MIL-101 and simulated MIL-101 from CIF file obtained from Cambridge Structure Database **b)** 1H NMR spectrum of the linker of MIL-101, NO₂-101, NH₂-101 and NHCOCH₃-101 measured in 2 wt.% NaOD/D₂O solution; These peaks 1,2,3 and 4 can be assigned to NHCOCH₃-H₂BDC, the integrals also fit well, NH₂-H₂BDC is marked by #,the peak at 4.79 ppm is attributed to residual water of NaOD/D₂O solvent; **c)** ESI-MS(negative mode) of digested and purified NHCOCH₃-101(Dissolved and diluted by methanol).

For NMR and EIS-MS test, the sample is digested by NaOD/D₂O to get a clear solution where the pH value is adjusted to 8~10 to precipitate Cr(OH)₃ (Note: >5wt.% NaOH aqueous solution can cause hydrolysis of NHCOCH₃-101 so low-concentration NaOH is necessary to collect NHCOCH₃-101 NMR spectra). In the NMR spectra, besides the presence of typical 1H chemical shift assigned to –CH₃, the downfiled shift compared with 1H resonance in amide-terephthalic acid (amide-H₂BDC) suggests the covalent introduction of secondary amide group, resulting in

the decrease in electronic density of aromatic 1H due to electrophilic amide group (Fig. S1(b)). The 1H peak integrity suggests the acylation yield from NH₂-101 to NHCOCH₃-101 is >80 %, agreeing with the reported results (*e.g.* IRMOF-3 and Uio-66).^{5,6} The negative mode ESI-MS obtained present a base peak at m/z=222.9, which corresponds to the amide-H₂BDC ligand (Fig. S1(c)).

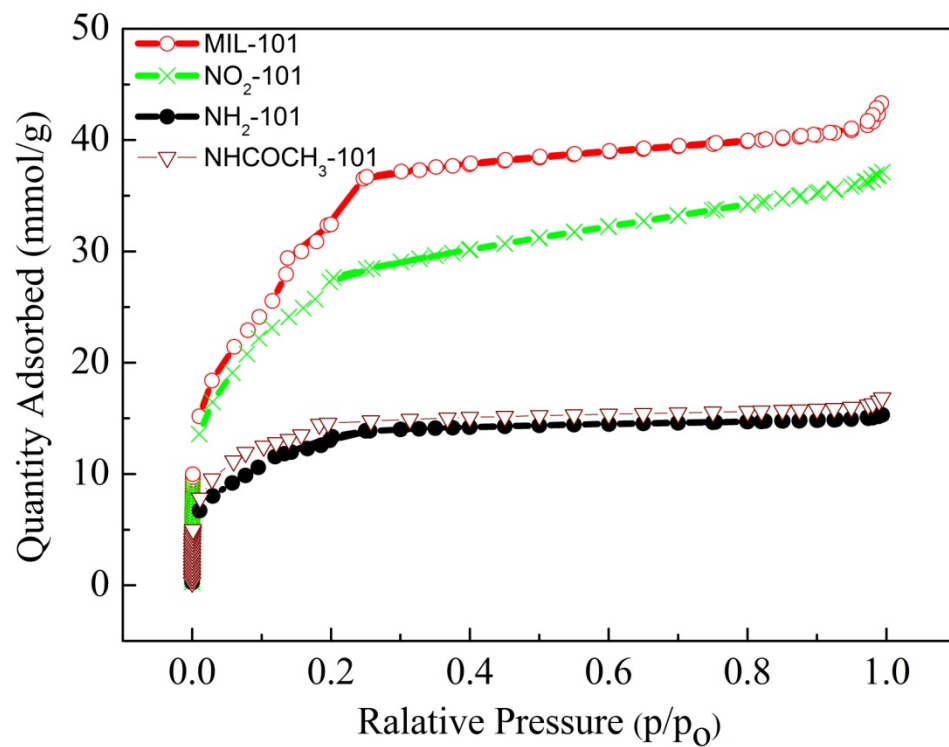


Figure S2. N₂ isothermal sorption curves at 77K for MIL-101(red line), NO₂-101(green line), NH₂-101(black line) and NHCOCH₃-101(purple line).

Table S1 Pore volumes and surface areas of MIL-101 and various functionalized MIL-101s determined by N₂ sorption.

MOFs	Pore volume(cm ³ /g)	Surface area(m ² /g)
MIL-101	1.43	2882
NO ₂ -101	1.25	2252
NH ₂ -101	0.52	1087
NHCOCH ₃ -101	0.56	1186

Table S2. The peak hydrogen release temperature for AB-MIL-101s composites prepared *via* impregnation and grinding methods and the hydrogen release weight percentage based on the total AB/MOFs mass. Peak temperature for hydrogen release for neat AB is 110 °C.

Composites	Peak temperature (°C) for hydrogen release		Hydrogen release amount (wt. %) ^a	
	Impregnation	Grinding	85°C	200 °C
AB		110	0.4	9.6
AB-101	87	101	4.9	6
AB-NO ₂ -101	88/104	105	3.8	5.7
AB-NH ₂ -101	73	87	5.6	8.3
AB-NHCOCH ₃ -101	87	94	5.3	7.9

^a: Based on the total AB and MOFs mass, not only based on the AB alone.

Table S3. The density of MIL-101, functionalized MIL-101 and AB-MIL-101s measured by pycnometer where dodecane was used as suspension agent.

Sample	Density (g/mL)
AB	0.78
MIL-101	0.62
AB-MIL-101	0.88
NO ₂ -101	0.71
AB-NO ₂ -101	0.79
NH ₂ -101	0.65
AB-NH ₂ -101	0.74
NHCOCH ₃ -101	0.73
AB-NHCOCH ₃ -101	0.94

Table S4. Effective gravimetric and volumetric hydrogen storage of AB impregnated into MOFs.

Sample	Effective hydrogen storage value on a materials basis ^a			
	Release @ 85 °C		Release @ 200 °C	
	Gravimetric value (g H ₂ /kg)	Volumetric value (g H ₂ /L) ^b	Gravimetric value (g H ₂ /kg)	Volumetric value (g H ₂ /L) ^b
AB	4	3	96	74
AB-MIL-101	49	43	60	52
AB-NO ₂ -101	38	30	57	45
AB-NH ₂ -101	56	41	83	61
AB-NHCOCH ₃ -101	53	48	79	72

^aThis value is calculated based on AB-MIL-101s amount, not only AB alone.

^bThe sample density is determined by a pycnometer method, where dodecane as a suspending agent: AB: 0.78 g/mL; AB-MIL-101: 0.88 g/mL; AB-NO₂-101: 0.79 g/mL; AB-NH₂-101: 0.74 g/mL; AB-NHCOCH₃-101: 0.91g/mL.

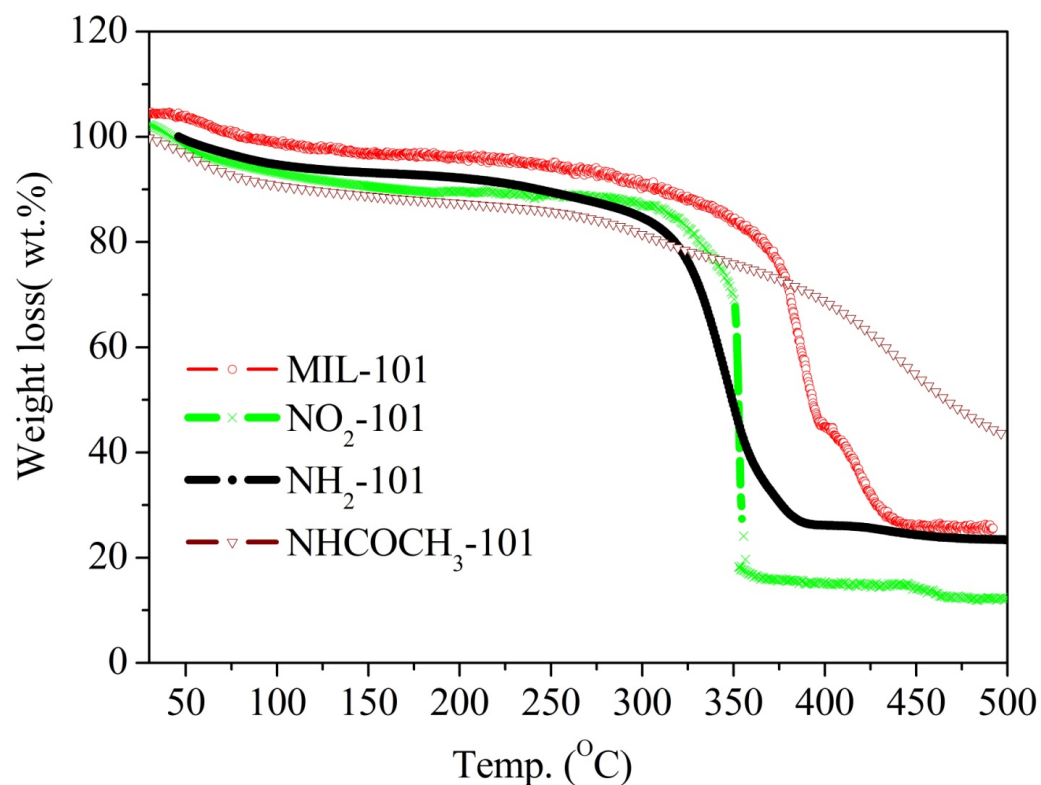


Figure S3 TGA curves between 40 and 500 °C for MIL-101 and its functionalized derivative (20 mL/min N₂ flow and 3 °C/min).

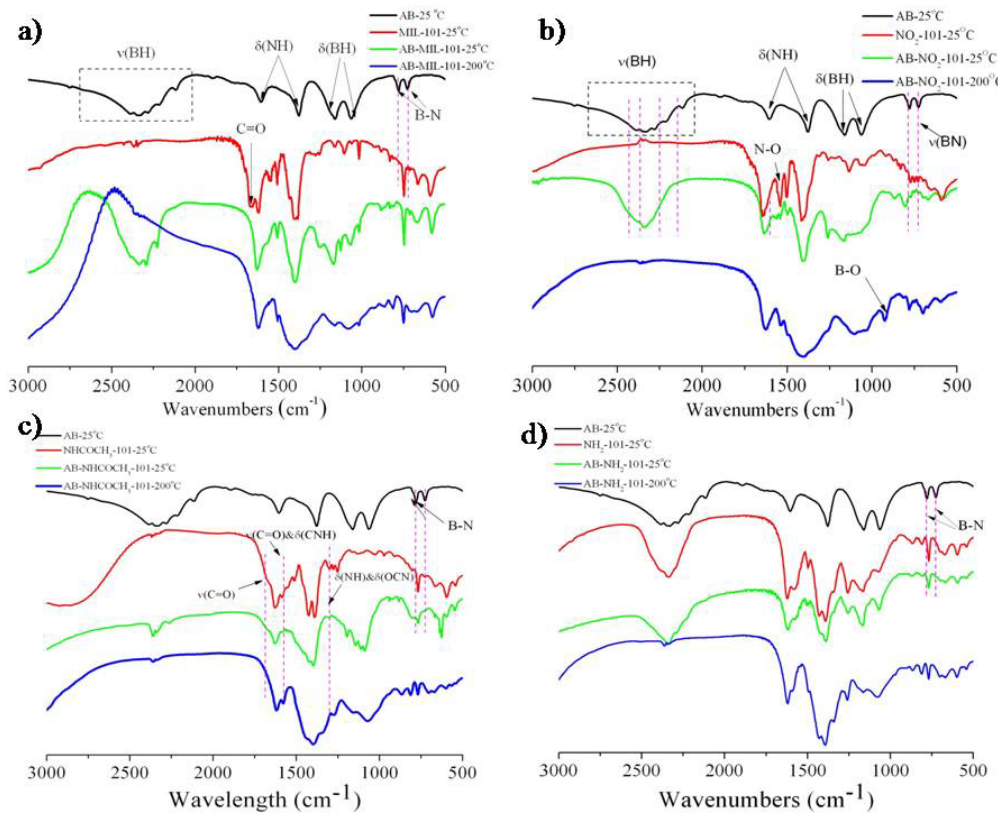


Figure S4. FTIR spectra of different types of MOFs before (red line) and after (green line) mixing with AB, and further heat treatment at 200 °C(blue line): (a) MIL-101 untreated; (b)NO₂-101; (c)NH₂-101 and(d)NHCOCH₃-101.

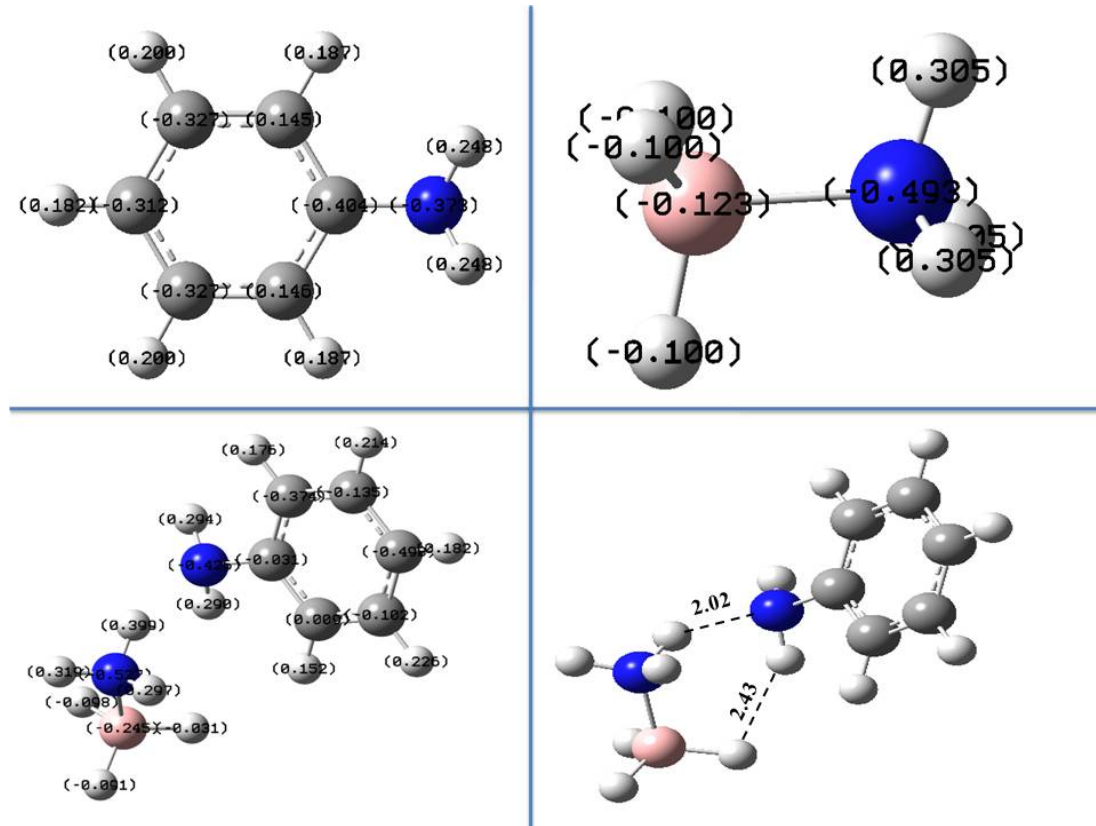


Figure S5 Muliken population analysis of charge densities and low-energy structure of AB, $\text{NH}_2\text{-H}_2\text{BDC}$, AB- $\text{NH}_2\text{-BDC}$.

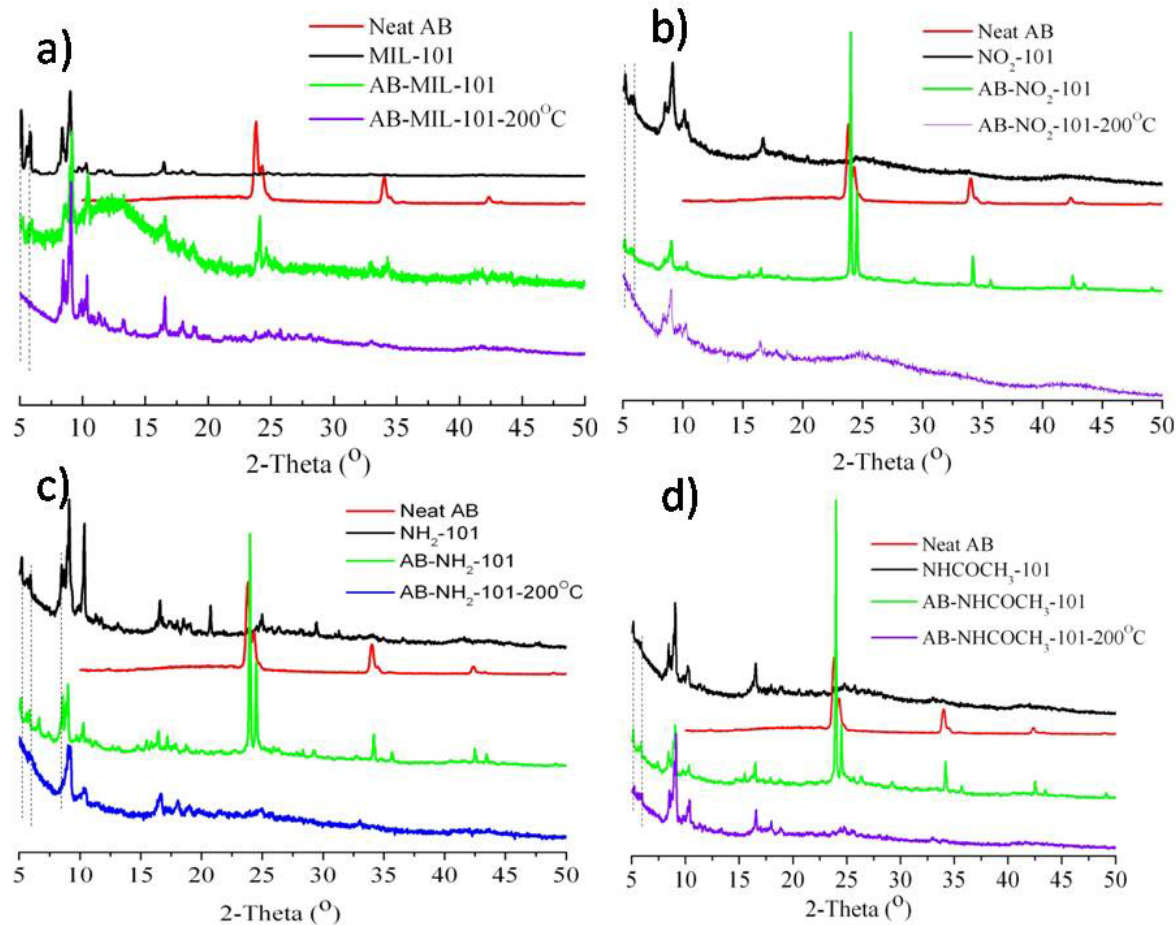


Figure S6. XRD patterns for various functionalized MIL-101s (black line), neat AB (in red line) and AB/functionalized MIL-101s systems (green line)

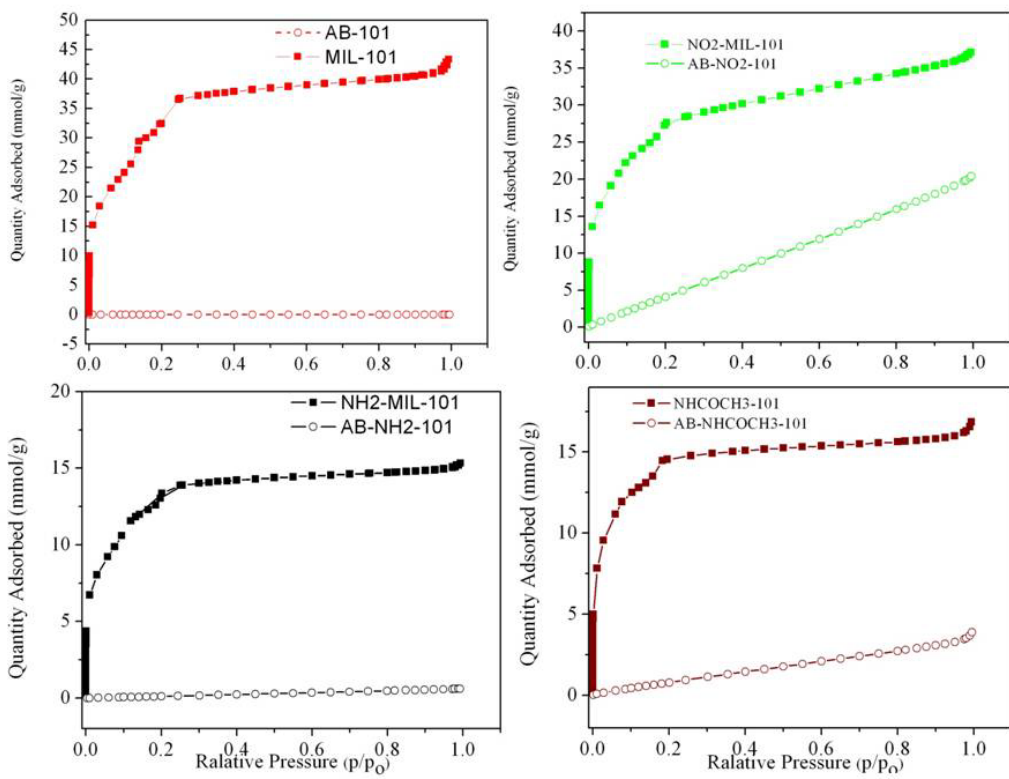


Figure S7. N₂ isothermal sorption for functionalized MOFs and AB/functionalized MOFs.

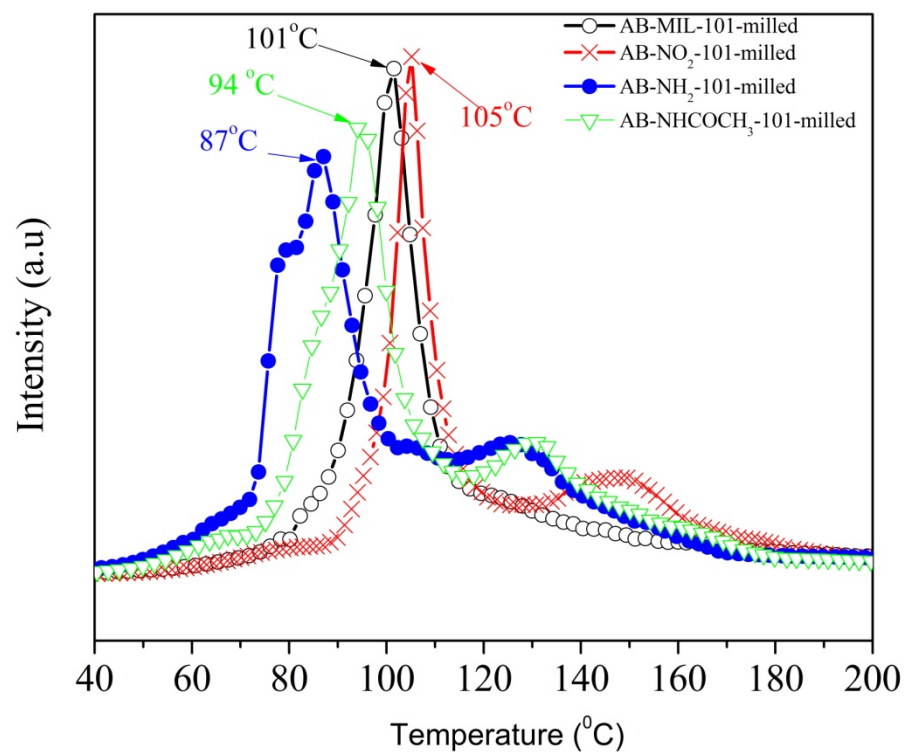


Figure S8.H₂ TPD/MS for AB/MIL-101s mixtures, which are prepared by grinding 1:1 wt/wt AB and MIL-101s in a mortar for 10 mins. These data indicates that the functionalized MIL-101(Cr) can interact with AB to decrease its dehydrogenation temperature without nanoconfinement.

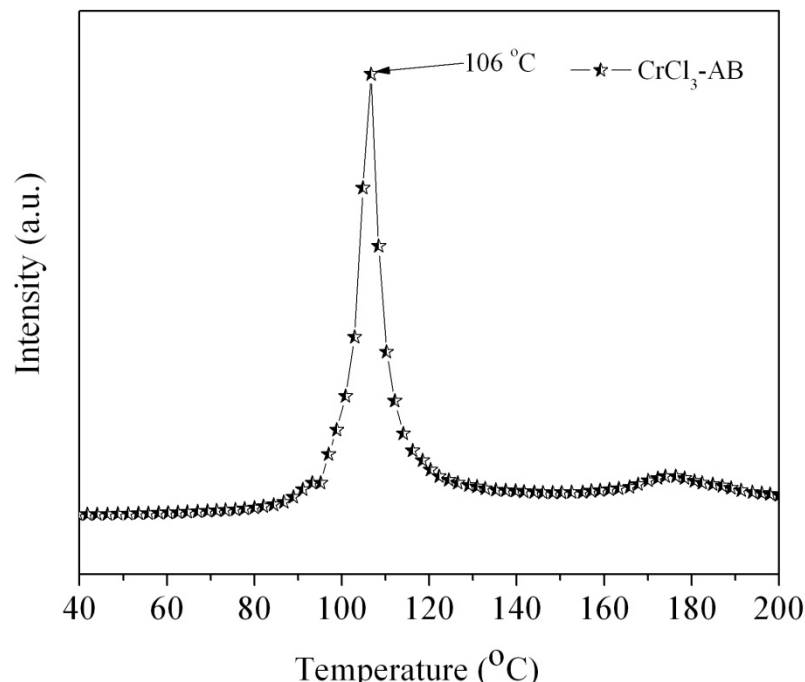


Figure S9. H₂ TPD/MS for CrCl₃ and AB mixture, which are prepared by grinding 1:1 wt/wt AB and CrCl₃ in a mortar for 10 mins. This data indicates that the Cr metal ion cannot significantly decrease AB dehydrogenation temperature.

References

1. G. Férey, C. Mellot-Draznieks, C. Serre, F. Millange, J. Dutour, S. Surblé and I. Margiolaki, *Science*, 2005, **309**, 2040-2042.
2. S. Bernt, V. Guillerm, C. Serre and N. Stock, *Chem. Comm.*, 2011, **47**, 2838-2840.
3. J. Kotaś and Z. Stasicka, *Environ. Pollut.*, 2000, **107**, 263-283.
4. R. C. Gaussian 03, M. J. Frisch, G. W. Trucks, H. B. Schlegel, G. E. Scuseria, M. A. Robb, J. R. Cheeseman, J. A. Montgomery, Jr., T. Vreven, K. N. Kudin, J. C. Burant, J. M. Millam, S. S. Iyengar, J. Tomasi, V. Barone, B. Mennucci, M. Cossi, G. Scalmani, N. Rega, G. A. Petersson, H. Nakatsuji, M. Hada, M. Ehara, K. Toyota, R. Fukuda, J. Hasegawa, M. Ishida, T. Nakajima, Y. Honda, O. Kitao, H. Nakai, M. Klene, X. Li, J. E. Knox, H. P. Hratchian, J. B. Cross, V. Bakken, C. Adamo, J. Jaramillo, R. Gomperts, R. E. Stratmann, O. Yazyev, A. J. Austin, R. Cammi, C. Pomelli, J. W. Ochterski, P. Y. Ayala, K. Morokuma, G. A. Voth, P. Salvador, J. J. Dannenberg, V. G. Zakrzewski, S. Dapprich, A. D. Daniels, M. C. Strain, O. Farkas, D. K. Malick, A. D. Rabuck, K. Raghavachari, J. B. Foresman, J. V. Ortiz, Q. Cui, A. G. Baboul, S. Clifford, J. Cioslowski, B. B. Stefanov, G. Liu, A. Liashenko, P. Piskorz, I. Komaromi, R. L. Martin, D. J. Fox, T. Keith, M. A. Al-Laham, C. Y. Peng, A. Nanayakkara, M. Challacombe, P. M. W. Gill, B. Johnson, W. Chen, M. W. Wong, C. Gonzalez, and J. A. Pople, Gaussian, Inc., Wallingford CT, 2004.
5. Z. Wang and S. M. Cohen, *J. Am. Chem. Soc.*, 2007, **129**, 12368-12369.
6. M. Kandiah, S. Usseglio, S. Svelle, U. Olsbye, K. P. Lillerud and M. Tilset, *J. Mater. Chem.*, 2010, **20**, 9848-9851.